

Modelling the behavior of human crowds with interacting particle systems in active-passive population dynamics

Thi Kim Thoa Thieu^{a,*}, Roderick Melnik^{a,b}

^a*M3AI Laboratory, MS2Discovery Interdisciplinary Research Institute, Wilfrid Laurier
University,*

75 University Ave W, Waterloo, Ontario, Canada N2L 3C5

^b*BCAM - Basque Center for Applied Mathematics, Bilbao, Spain
Email: {tthieu, rmelnik}@wlu.ca*

Abstract

The modelling of human crowd behaviors offers many challenging questions to science in general. Specifically, the social human behavior consists of many physiological and psychological processes which are still largely unknown. To model reliably such human crowd systems with complex social interactions, stochastic tools play an important role for the setting of mathematical formulations of the problems. In this work, using the description based on an exclusion principle, we study a statistical-mechanics-based lattice gas model for active-passive population dynamics with an application to human crowd behaviors. We provide representative numerical examples for the evacuation dynamics of human crowds, where the main focus in our considerations is given to an interacting particle system of active and passive human groups. Furthermore, our numerical results show that the communication between active and passive humans strongly influences the evacuation time of the whole population even when the “faster-is-slower” phenomenon is taken into account. Finally, to provide an additional inside into the problem, a stationary state of our model is analyzed via current representations and heat map techniques.

Keywords: Crowd dynamics, Collective behavior, Faster-is-slower, Particles

☆

*Corresponding author

January 19, 2022

1. Introduction

Social dynamics and human behavior are closely connected. Moreover, the detailed behavior of human crowds is already complicated, being caused by many physiological, sociological and psychological processes, and it is still largely unknown. The topic of human crowds offers many challenging questions to the scientific community. In crowd dynamics studies, the movements of human groups must directly be related to their decision making processes. Hence, the characteristics of human flows are apparently affected by decisions of each individual in the group. This influence needs to be accounted for in order to model the processes properly. In an emergency situation, in particular in urban areas [1, 2, 3, 4], individuals require information about surrounding environment and social interactions in order to evacuate successfully. Therefore, stochastic models and tools become important to capture the essence of the interactions among such individuals (e.g. [5, 6, 7]). One of the most promising routes in this direction is the development of statistical-mechanics-based lattice gas system models for the dynamics of active-passive populations. In general, contributions from psychology are also needed to model the dynamics of emotional behaviors which can affect the human strategy. Likewise, contributions from neuroscience may also be vital to better understand the collective learning dynamics of people that face emergency situations [8, 9]. By now we know that the emergence of collective opinions in a multi-agent system brings about a challenging situation when it comes to modelling complex biosocial systems [10, 11]. The formation of (partial) consensus among agents can lead to such collective opinions in many cases [12]. There are a number of relevant results available on the topics of the behavior of human crowds. In particular, a relevant result on dissonance minimization as a micro foundation of social influence in models of opinion formation has been reported in [13], where the authors show that differ-

ent models of opinion formation can be represented as best response dynamics within a general framework of social influence. A model for dynamics of conflicting opinions considering rationality has been studied in [14]. In [15], the authors experimentally investigated the effect of different proportions of patient (no-rush) versus impatient (rush) individuals in an evacuating crowd. A multiscale vision of human crowd models, which provides a consistent description at the three possible modelling scales, namely, microscopic, mesoscopic, and macroscopic, has been reported in [16]. At the application level, the authors of [17] developed a model within a multiscale framework accounting for the interaction of different spatial scales, from the small scale of the SARS-CoV-2 virus itself and cells, to the large scale of individuals and further up to the collective behaviour of populations. One of the most common phenomena in crowd dynamics is the phenomenon of self-organization. It is worth pointing out that human crowds are able to produce coherent flow patterns, and demonstrate manifestations of certain built-in self-organization mechanisms. For example, as shown in [18, 19], pedestrian flows, either uniform or not, can form collective patterns of motion. For instance, one notices circulating flows at intersections, crowd flows at bottlenecks, lane formations, local cloggings due to a complex geometry [20, 21]. These behaviors are typically caused by walls and obstacles under normal walking conditions, including the situations when the evacuation of pedestrians takes place during an emergency situation. Furthermore, the well-known “faster-is-slower” effect is an important instance of self-organized phenomenon in crowd dynamics [22, 23, 24]. In general, the “faster-is-slower” effect is caused by the impatience of human groups with panic moods in an emergency situation. Another example is provided by the clogging of humans at an exit door or a bottleneck that could lead to fatal accidents. A better understanding of the “faster-is-slower” phenomenon would help to avoid unexpected accidents and reduce the evacuation time of human groups in emergency scenarios.

In this paper, we study an interacting particle system, modelling the dynamics of a mixed group of active-passive particles with applications to human

crowd behaviors. We provide representative numerical examples of an evacuation dynamic of active-passive human groups. In particular, we focus on the situation where an active human group is aware of the details of the environment and move towards the exit door, while a passive population is not aware of the details of the geometry and move randomly to explore the environment and eventually to find the exit. In this context, humans interact by communicating between active and passive human groups. Specifically, the active human group transfers the information of surrounding environment to the passive human group. We give our special attention to representative numerical examples on the evacuation dynamics of such active-passive human groups, where we observe a classical “faster-is-slower” effect. Furthermore, a stationary state of our model is also investigated, with corresponding current and heat map characteristics discussed in detail.

2. Model description

Our starting point is a crowd dynamics model for active-passive particles. This particle system is considered within the geometry confined to a square lattice $\Lambda := \{1, \dots, L\} \times \{1, \dots, L\} \subset \mathbb{Z}^2$ of side length L , where L is an odd positive integer number. In the examples that follow the lattice Λ can be interpreted as a *room*, where a point $x = (x_1, x_2)$ of the room Λ is called a *site*. When two sites x, y are at the Euclidean distance one, i.e. $|x - y| = 1$, we call them *nearest neighbors*. The “door” is represented as a set made of $w_{\text{ex}} = \omega$ pairwise adjacent sites, with $\omega < L$ being an odd positive integer, located on the top row of the room Λ and symmetric with respect to its median column. This representation of the door can be considered as an exit door with its *width* ω of the exit. We denote by N_A the total number of active particles, and by N_P the total number of passive particles with $N := N_A + N_P$ and $N_A, N_P, N \in \mathbb{N}$.

Furthermore, we define a rectangular interaction zone V (*visibility region*) inside the top part of the room Λ . This visibility zone is made of the first L_v top rows of Λ , where the positive integer $L_v \leq L$ called *depth* of the visibility region,

see in Fig. 1. We refer to the case in which no visibility region is considered by writing $L_v = 0$.

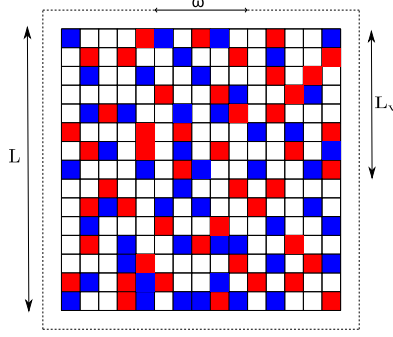


Figure 1: (Color online) Schematic representation of our lattice model with size L . Blue and red squares represent passive and active particles, respectively, while the white squares within the geometry denote the empty spots. The reflecting boundary conditions is represented by the thick dashed line surrounding a large fraction of the grid. An exit door is located in presence of the arrow, with its width equal to ω . The visibility region with the length $L_v \leq L$ is represented in the geometry.

In the remainder of this section, we highlight several key points important in further analysis. We focus on two different species of *active* and *passive* particles, moving inside Λ and we use two symbols A and P to respectively refer to them. Note that particles cannot access the sites of the external boundary of the room, i.e. there are sites $x \in \mathbb{Z}^2 \setminus \Lambda$ such that there exists $y \in \Lambda$ nearest neighbor of x . We call the occupation number η_x and the state of the system *configuration* $\eta \in \Omega = \{-1, 0, 1\}^\Lambda$, where we have:

$$\begin{cases} \eta_x = 0, & \text{if the site } x \text{ is } \textit{empty}, \\ \eta_x = 1, & \text{if the site } x \text{ is } \textit{occupied by an active particle}, \\ \eta_x = -1, & \text{if the site } x \text{ is } \textit{occupied by a passive particle}. \end{cases}$$

Furthermore, the quantities $n_A(\eta) = \sum_{x \in \Lambda} \delta_{1, \eta_x}$ and $n_P(\eta) = \sum_{x \in \Lambda} \delta_{-1, \eta_x}$ represent the numbers of active and passive particles in the configuration η , respectively, with $\delta_{\cdot, \cdot}$ being the Kronecker symbol. The total number of particles in

the configuration η is the sum of $n_A(\eta)$ and $n_P(\eta)$.

The overall dynamics of our system can be represented by the continuous time Markov chain $\eta(t)$ on Ω with rates $c(\eta, \eta')$ defined as in [5]. Markov chains provide a well-established tool for modelling complex dynamic evolution, including the situations where multiscale features of the dynamics have to be accounted for [25, 26, 27, 28]. Based on our Markov chain representation, we are now in a position to analyze the dynamics of our active and passive human groups. In this case, using a simple exclusion process, the underlying dynamics can be modelled as follow: the passive population performs a symmetric simple exclusion dynamics on the whole lattice, whereas the active population is subject to a drift, guiding particles towards the exit door.

In our model, let $\varepsilon \geq 0$ be the *drift*. We assume that only active particles experience the drift, changes of the parameters L_v and ε act directly only on the active species, while passive particles do not depend on the drift value.

The above construction follows the ideas originally discussed in [5, 6]. In these earlier works, the interaction of particles inside the room was modelled via a simple exclusion random walk for two particle species undergoing two different microscopic dynamics. The passive particles performed a symmetric simple exclusion dynamics on the whole lattice, while the active particles performed a symmetric simple exclusion walk outside the visibility region, whereas inside such a region they experienced a drift pushing them towards the exit. The active particles were obscure only in the region outside the visibility region, while the whole lattice was obscure for the passive particles. In our current consideration, motivated by the recent results of [7], we have modified this earlier model by incorporating the interaction between active and passive particles and analyzing it on an example of modelling the dynamics of a mixed group of active-passive humans. In particular, we assume that a passive human can communicate with active humans at his nearest neighbor sites. After receiving enough information from the active humans, the passive human becomes active and has the same behavior as the active one. Further details of the underlying scheme and its numerical implementation are provided in Section 3.

3. Numerical results

In this section, we consider an application of our interacting particle system, modelling the dynamics of human groups. In particular, we investigate an interacting particles system of active and passive populations on the example of interacting active and passive human groups. We assume that active particles can be seen as active humans while passive particles can be considered as passive humans and both human groups wish to escape the room due to an emergency situation. The underlying dynamic process can be described as follows: the active humans have the information about the geometry (knowing the location of the exit door) and automatically transfer the information to the passive human group. After receiving the information from the active human group, the passive humans follow the active human group. Hence, the passive humans are “switched” to active humans. At this moment, we assume that the passive human group trusts the active human group by communicating with active humans at its nearest neighbor sites. Moreover, we assume that the drift quantity ε represents the level of panic mood measuring the need of escaping the room in an emergency situation. In particular, the larger ε of active humans, the more active humans wish to get out of the room.

The numerical results reported in this section are obtained by using the kinetic Monte Carlo (KMC) method. The methodology is effectively based on a dynamic Monte Carlo technique and follows in its essence [5], where a lattice-gas-type version of KMC was applied to the study of pedestrian flows. In particular, we use the scheme in Fig. 2 to simulate the presented model. Note that as in all KMC versions, we need to define the rate $c(\eta(t), \eta)$, which is done here in the same manner as in [5].

In the current version of the algorithm, we consider the communication between active and passive human groups by using the same techniques as in [7]. In particular, each site on the lattice is connected by edges and the connectivity between these edges at one site is known as the degree of the site denoted by $\deg(i, j)$, see Fig. 3. The last part of the algorithm operates as follows. If an

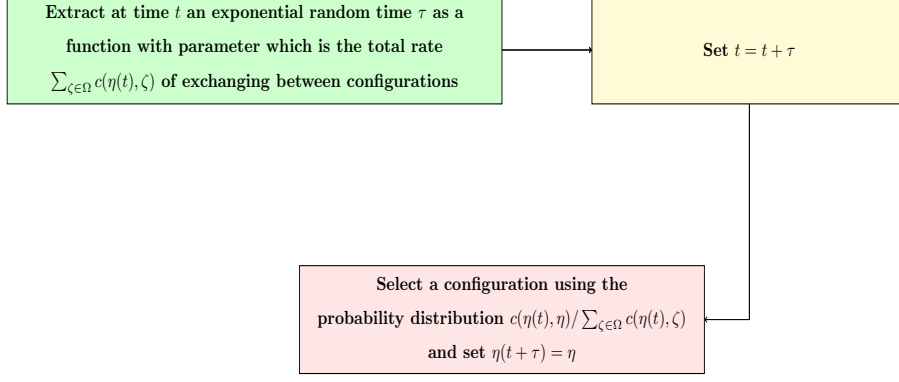


Figure 2: Key dynamic steps in the KMC numerical scheme implementation based on the continuous Markov chain $\eta(t)$.

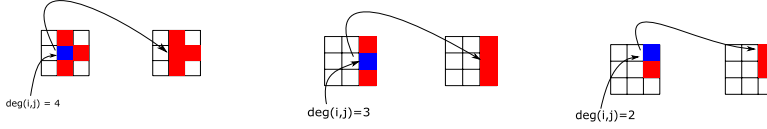


Figure 3: (Color online) Schematic representation of the interaction between active and passive particles.

arrival site (i, j) on the lattice is occupied by a passive particle, then we count the total number of active particles at its nearest neighbor sites. If the total number of actives particles is equal to $\deg(i, j) - 1$ at its nearest neighbor sites, then the passive particle is switched to the active one. Note that an arrival site of a site x here is the random site chosen among possible empty sites at nearest neighbor sites of x . We expect that after communicating between active-passive human groups, almost all passive particles become active. Then, this seems to help the whole population in the room escape faster. The overall picture of our human crowd dynamics model is illustrated in Fig. 4, where we show the configurations of the system at different times.

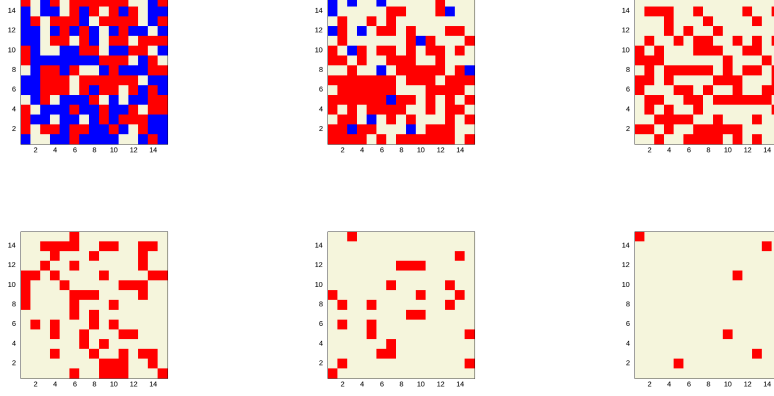


Figure 4: [From passive to active] Configurations of the model at different times (increasing in lexicographic order) with parameters: $L = 15$, $w_{\text{ex}} = 7$, and $\varepsilon = 0.3$. Red pixels represent active particles, while blue pixels denote passive particles, and gray sites are empty. In the initial configuration (top left panel) there are 90 active and 90 passive particles.

3.1. The evacuation time

Considering the dynamics defined in Section 2, we define τ_η as the following first hitting time to the empty configuration (e.g. [5]):

$$\tau_\eta = \inf\{t > 0 : \eta(t) = \underline{0}\}, \quad (1)$$

for the chain started at $\eta \in \Omega$. Moreover, given a configuration $\eta \in \Omega$, the *evacuation time* starting from η is defined as the following formulation

$$T_\eta = \mathbb{E}_\eta[\tau_\eta]. \quad (2)$$

Here, the probability measure is induced by the Markov chain, described in Section 2, and \mathbb{E}_η is the corresponding expectation. Note that in the limit, one can introduce the infinitesimal generator $\mathcal{L}(\eta) = \sum_{\eta' \in \Omega} c(\eta, \eta')[f(\eta') - f(\eta)]$ acting on continuous bounded functions $f : \Omega \rightarrow \mathbb{R}$, see, e.g. [29, 30].

According to (2), we define the evacuation time here as the time needed to evacuate all the particles initially in the system. In other words, the evacuation

time is the time at which the last particle leaves the room. Next, we investigate the evacuation time of our human groups for a fixed initial random condition with specific values of the initial drift ε and visibility depth L_v .

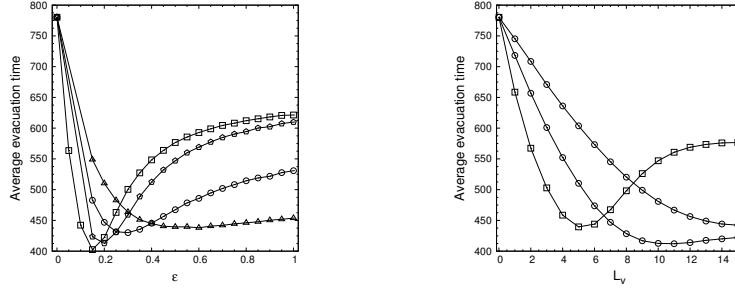


Figure 5: Evacuation time of active-passive human groups. Left panel: evacuation time of active-passive particles as a function of ε with $L_v = 5$ (open triangles), $L_v = 7$ (open circles), $L_v = 10$ (open pentagons), $L_v = 15$ (open squares). Right panel: evacuation time as a function of L_v with $\varepsilon = 0.1$ (open triangles), $\varepsilon = 0.15$ (open circles), $\varepsilon = 0.2$ (open pentagons), $\varepsilon = 0.5$ (open squares).

In the simulations, we fix the parameters for $L = 15$, $w_{\text{ex}} = \omega = 7$ and $N_A = N_P = 90$. The featured numerical results of our analysis are shown in Fig. 5, where we have plotted the evacuation time as a function of ε and L_v . These numerical results demonstrate that too “smart” humans increase the evacuation time. In the left panel of Fig. 5, for $L_v = 5$, when we increase the values of ε , the evacuation time decreases up to $\varepsilon \approx 0.45$, then stays the same and slightly increases from $\varepsilon = 0.8$ to 1. For $L_v = 7, 10, 15$, we note that the evacuation time reduces with ε up to some values where it attains a minimum. However, soon after the evacuation time reaches its minimum, it increases significantly with the position and the size of the minimum change, respectively. This behavior is interesting since we expect that after the communication is included into consideration, the whole population should be able to escape faster. However, the presence of such a large visibility depth and drift quantity can increase the evacuation time of the whole population. This is due to the fact that after the communication between active and passive humans takes place, almost all passive humans become active humans. Moreover, all active humans are subject

to a drift, guiding the active human group toward the exit door. Therefore, there is an accumulation of humans at the exit door that increases the evacuation time. This phenomenon is also demonstrated by the right panel of Fig. 5. The numerical results that we observe here are a consequence of what is known as the “faster-is-slower” effect. Normally, the “faster-is-slower” effect is caused by the impatience of people in a panic mood. When people try to move faster, their average evacuation time increases. The accumulation of humans can cause clogging at an exit or a bottleneck that could lead to fatal accidents. This effect can be particularly tragic in the presence of fires, where fleeing people can reduce their own chances of survival [18].

As the next step, it is worth analyzing our system at the stationary state, which should provide further insight into the behavior we consider here.

3.2. The stationary occupation number profiles

In this subsection, we examine the stationary state of our model following the ideas of an analysis discussed in [6]. In particular, we modify the model presented in Section 2 by considering the room with two doors, top and bottom. The bottom door, located at the bottom row of the lattice Λ , is symmetric with respect to its median column. It has the same width as the top door. We assume that every “particle” exiting the domain via the top door is introduced back at one site randomly chosen among possible empty sites of the bottom door, see Fig. 6. Then, the system will reach a stationary state. Note that there is a slight fluctuation in the total number of active and passive particles due to the fact that particles may enter waiting lists during evolution. Moreover, the total number of particles N in the system is conserved by considering both the room and the waiting lists.

We shall consider *occupation number profiles* of active and passive particles, i.e. we evaluate the stationary mean value of the occupation numbers of active and passive particles. We assume that active-passive particles move inside the lattice Λ with the following rates:

- a passive particle leaves the room from a site in the top door with rate 1;

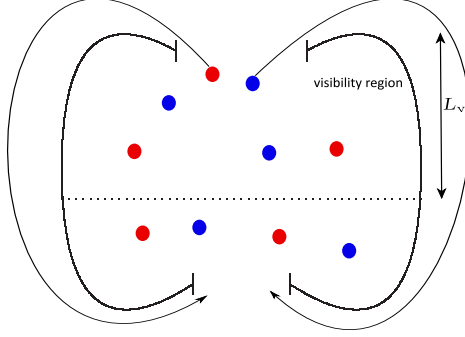


Figure 6: (Color online) Qualitative description of our model: red dots represent active particles, blue dots represent passive particles. Active particles are subject to a drift, guiding particles toward the exit door in the visibility zone. Outside the visibility region all particles are moving isotropically. All particles leave the room via the top exit door are introduced back to the system via an entrance door at the bottom of the geometry.

- an active particle leaves the room from a site in the top door with rate $1 + \epsilon(x, y)$;
- if $n_A < N_A$ and $m_B \neq 0$, then an active particle is added to a randomly chosen empty site of the bottom door with rate $[N_A - n_A]/m_B$;
- if $n_P < N_P$ and $m_B \neq 0$, then a passive particle is added to a randomly chosen empty site of the bottom door with rate $[N_P - n_P]/m_B$;
- a passive particle moves inside Λ from a site to one of its empty nearest neighbors with rate 1;
- an active particle moves inside Λ from a site to one of its empty nearest site with rate $1 + \epsilon(x, y)$.

Here, n_A and n_P denote the numbers of active and passive particles in the room, respectively. The numbers of active and passive particles that exited the room and entered their own waiting lists at the considered time are represented by the quantities $N_A - n_A$ and $N_P - n_P$, respectively. Moreover, $m_B > 0$ is the number of empty sites of the bottom door at the same time.

In the study of these dynamic processes, one of the main quantities of interest is the stationary *outgoing flux* or *current of active and passive particles*. The current is defined in the infinite time limit by the ratio between the total number of active and passive particles, that in the interval $(0, t)$ exited through the top door to enter the waiting lists, and the time t . In order to better understand the behavior of currents with respect to the model parameters, we shall also look at the *occupation number profiles* of active and passive particles. Using the same methodology as in [6], we will evaluate the stationary mean value of the occupation numbers of active and passive particles.

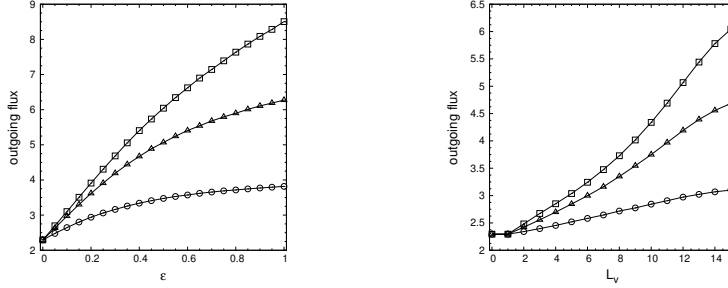


Figure 7: Stationary current for the case of communication between active-passive populations. Left panel: $L_v = 7$ (empty circles), $L_v = 12$ (empty triangles), $L_v = 15$ (empty squares). Right panel: $\epsilon = 0.1$ (empty circles), $\epsilon = 0.3$ (empty triangles), $\epsilon = 0.5$ (empty squares)

In the simulations, we fix the parameters for $L = 15$, $w_{\text{ex}} = \omega = 7$ and $N_A = N_P = 90$. The featured numerical results of our analysis here are shown in Figs. 7-10. In Fig.6, we plotted the stationary currents as functions of ϵ and L_v . We observe that the behavior of the currents of active-passive humans demonstrates an expected pattern, in which the currents increase monotonically both with respect to the drift quantity and the length of the visibility region. In particular, in the left panel of Fig.6, when we increase the values of ϵ , the currents of active-passive humans increase significantly. Moreover, the current of active-passive humans in the case of $L_v = 7$ is smaller than in the cases of $L_v = 12$ and $L_v = 15$. This is also evident from in the right panel, where the currents increase when we increase the values of L_v .

In order to analyze this effect further, we look at the corresponding occupation number profile, obtained from our model. In what follows, we use a data visualization technique known as heat maps [31]. As seen from Figs. 8 - 10, active humans are mainly distributed at their exit door. This is observable in all of the panels in these figures. For large values of ε and L_v , due to the transverse component of the drift, there is an accumulation of particles in the central part of the room. Moreover, it is clear that particles can form a central “droplet” detached from the “inlet” top door depending on the length of the visibility region.

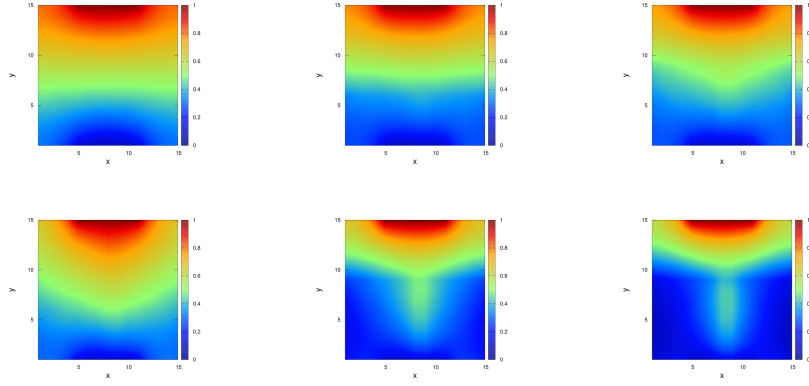


Figure 8: Heat maps (different values of ε) for the case of interaction between active-passive humans: $L_v = 7$ and $\varepsilon = 0$, $L_v = 7$ and $\varepsilon = 0.1$, $L_v = 10$ and $\varepsilon = 0.1$, $L_v = 15$ and $\varepsilon = 0.1$, $L_v = 10$ and $\varepsilon = 0.3$, $L_v = 10$ and $\varepsilon = 0.5$.

3.3. Comparison with the case without interaction between active-passive particles

In this section, we compare the evacuation times in two different situations: with and without communication between active and passive humans. In the simulations, we fix the parameters for $L = 15$, $w_{\text{ex}} = \omega = 7$ and $N_A = N_P = 90$. The featured numerical results from our analysis in this subsection are shown in Fig. 11, where we have plotted the evacuation time as a function of ε and L_v for the two considered cases, with and without communication

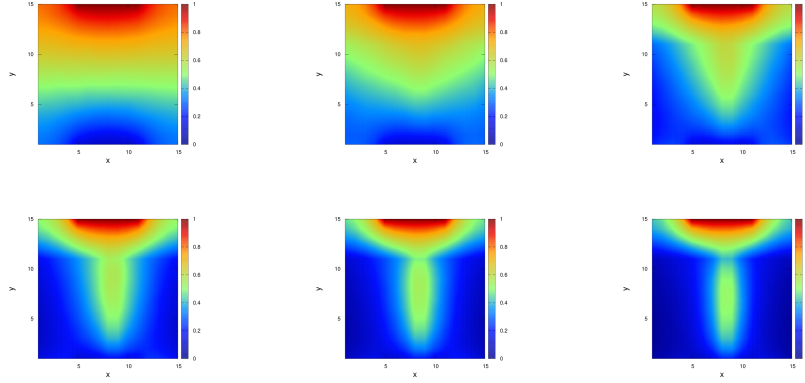


Figure 9: Heat maps (different values of ε) for the case of interaction between active-passive humans $L_v = 12$.

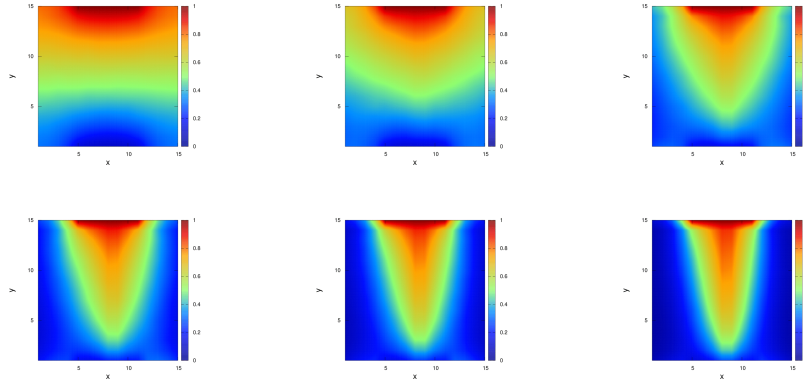


Figure 10: Heat maps (different values of ε) for the case of interaction between active-passive humans $L_v = 15$.

between active-passive humans. In particular, in the left panel of Fig. 11, for $L_v = 7$ and $L_v = 15$, the average evacuation time without communication between active and passive humans is larger than the average evacuation time with communication between the two human groups when we increase the value of ε . Moreover, it is clear that even the average evacuation time in the dynamics with communication between active-passive humans reduces significantly up to some minimum values and then increases dramatically under suitable values of

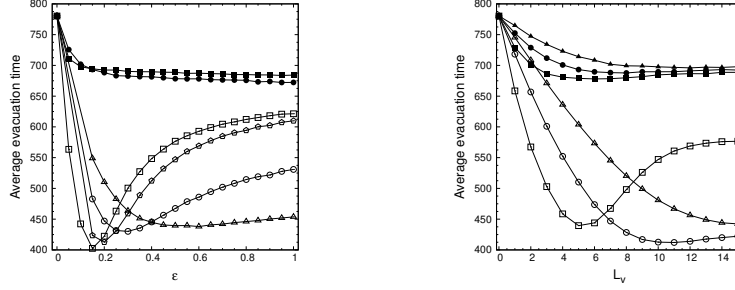


Figure 11: Evacuation time of active-passive human groups: no communication between active-passive human groups (solid disks), with communication between active-passive human groups (open symbols). Left panel: evacuation time of active-passive particles as a function of ε with $L_v = 5$ (open triangles), $L_v = 7$ (open circles), $L_v = 10$ (open pentagons), $L_v = 15$ (open squares). Right panel: evacuation time as a function of L_v with $\varepsilon = 0.1$ (open triangles), $\varepsilon = 0.2$ (open circles), $\varepsilon = 0.5$ (open squares).

ε and L_v . The average evacuation time with communication between active-passive humans is still smaller than in the case without communication between the two groups. Hence, the communication between active and passive humans strongly affects the evacuation time of the whole populations. This is visible also in the right panel, for $\varepsilon = 0.1, 0.2, 0.5$, when we increase the values of L_v . Indeed, the evacuation time in the dynamics of exchanging information between active and passive humans is smaller than in the case without communication between the two human groups. Even for large enough value of $\varepsilon = 0.5$ and L_v from 5 to 15, the evacuation time in the dynamics of switching from passive to active humans is still smaller than in the case when there is no exchange of the information between active and passive populations. Finally, it is worth noting that the communication between active and passive humans strongly affects the evacuation time of the whole population even in the presence of a classical “faster-is-slower” phenomenon. Note also that in the dynamics without communication, there is the presence of only a simple exclusion constraint of the lattice gas dynamics. This special case has been reported in [5].

4. Conclusions

We have proposed and described a statistical-mechanics-based lattice gas model for active-passive populations, focusing on the application of human crowd behaviors in critical situations. Specifically, we have deduced the average evacuation time of active-passive human groups, where we have observed a classical “faster-is-slower” effect. Our numerical results have shown that the communication between active and passive human groups strongly influences the evacuation time of the whole population even in the presence of a standard “faster-is-slower” phenomenon. Moreover, we have investigated the stationary state of our model. In particular, the numerical results have demonstrated that the drift quantity and the length of the visibility region strongly affect the shape of the region where active humans accumulate. In general, the “faster-is-slower” effect and clogging at the narrow exits are not well understood due to their real-world complexity, and this contribution sheds light on these important issues. As a continuation of this work, it would be instructive to further investigate such bottleneck situations during emergency, since the instant herding behaviour of humans at the exit could lead to fatal accidents. Finally, we note that the ideas presented in this contribution may be extended to a system of coupled Langevin equations to observe the detailed dynamics of active-passive particles at the exit door.

Acknowledgment

Authors are grateful to the NSERC and the CRC Program for their support. RM is also acknowledging support of the BERC 2018-2021 program and Spanish Ministry of Science, Innovation and Universities through the Agencia Estatal de Investigacion (AEI) BCAM Severo Ochoa excellence accreditation SEV-2017-0718 and the Basque Government fund AI in BCAM EXP. 2019/00432.

References

- [1] S. Bretschneider, *Mathematical Models for Evacuation Planning in Urban Areas*, Springer, 2013.
- [2] Y. Shin, S. Kim, I. Moon, Simultaneous evacuation and entrance planning in complex building based on dynamic network flows, *Applied Mathematical Modelling* 73 (2019) 545–562.
- [3] P. Kubera, J. Felcman, On the verification of the pedestrian evacuation model, *Mathematics* 9 (2021) Art. 1525.
- [4] E. Ronchi, Developing and validating evacuation models for fire safety engineering, *Fire Safety Journal* 120 (2021) Art. 103020.
- [5] E. N. M. Cirillo, M. Colangeli, A. Muntean, T. K. T. Thieu, A lattice model for active-passive pedestrian dynamics: a quest for drafting effects, *Mathematical Biosciences and Engineering* 17 (2019) 460–477.
- [6] E. N. M. Cirillo and M. Colangeli and A. Muntean and T. K. T. Thieu, When diffusion faces drift: consequences of exclusion processes for bi-directional pedestrian flows, *Physica D: Nonlinear Phenomena* 413 (132651).
- [7] T. K. T. Thieu, R. Melnik, Combining coupled Skorokhod SDEs and lattice gas frameworks for multi-fidelity modelling of complex behavioral systems, *Proceedings of the IX International Conference on Computational Methods for Coupled Problems in Science and Engineering, Coupled Problems* (2021), 12 pages, CIMNE, Barcelona, Spain.
- [8] B. G. Silverman, N. I. Badler, N. Pelechano, K. O’Brien, Crowd simulation incorporating agent psychological models, roles and communication, Retrieved from <https://repository.upenn.edu/hms/29> (2005).
- [9] A. Templeton, J. Drury, A. Philippides, Walking together: behavioural signatures of psychological crowds, *R. Soc. Open Sci.* 5 (2018) 180172.

- [10] B. Tadić, R. Melnik, Modeling latent infection transmissions through biosocial stochastic dynamics, *PLoS ONE* 15 (10) (2020) e0241163.
- [11] B. Tadić and R. Melnik, Microscopic dynamics modeling unravels the role of asymptomatic virus carriers in SARS-CoV-2 epidemics at the interplay between biological and social factors, *Computers in Biology and Medicine* 133 (2021) 104422.
- [12] P. L. Sreen, S. Lewandowsky, C. R. Sunstein, R. Hertwig, How behavioural sciences can promote truth, autonomy and democratic discourse online, *Nature Human Behaviour* 4 (2020) 1102–1109.
- [13] J. L. P. Groeber, F. Schweitzer, Dissonance minimization as a microfoundation of social influence in models of opinion formation, *Journal of Mathematical Sociology* 38 (2014) 147–174.
- [14] C. Wang, Dynamics of conflicting opinions considering rationality, *Physica A* 560 (2020) 125160.
- [15] H. R. L. Lee, A. Bhatia, J. Brynjarsdóttir, N. Abaid, A. Barbaro, S. Butail, Speed modulated social influence in evacuating pedestrian crowds, *Collective Dynamics* 5 (2020) 1–24.
- [16] B. Aylaj, N. Bellomo, L. Gibelli, A. Reali, A unified multiscale vision of behavioral crowds, *Mathematical Models and Methods in Applied Sciences* 30 (1) (2020) 1–22.
- [17] N. Bellomo, R. Bingham, M. A. J. Chaplain, G. Dosi, G. Forni, D. A. Knopoff, J. Lowengrub, R. Twarock, M. E. Virgillito, A multiscale model of virus pandemic: Heterogeneous interactive entities in a globally connected world, *Mathematical Models and Methods in Applied Sciences* 30 (8) (2020) 1591–1651.
- [18] D. Helbing, L. Buzna, A. Johansson, T. Werner, Self-organized pedestrian crowd dynamics: Experiments, simulations, and design solutions, *Transportation Science* 39 (1) (2005) 1–24.

- [19] F. S. P. E. Cristiani, A. Tosin, Modeling rationality to control self-organization of crowds: An environmental approach, *SIAM Journal on Applied Mathematics* 75 (2015) 605–629.
- [20] A. Schadschneider, W. Klingsch, H. Klüpfel, T. Kretz, C. Rogsch, A. Seyfried, Evacuation Dynamics: Empirical Results, Modeling and Applications, In: Meyers R. (eds) *Extreme Environmental Events*. Springer, New York, NY, 2011.
- [21] A. Tordeux, M. Chraïbi, A. Seyfried, A. Schadschneider, Prediction of pedestrian dynamics in complex architectures with artificial neural networks, *Journal of Intelligent Transportation Systems* 24 (6) (2020) 556–568.
- [22] H. Oh, J. Park, Main factor causing “faster-is-slower” phenomenon during evacuation: rodent experiment and simulation, *Scientific Reports* 7 (2017) 13724.
- [23] C. von Krüchten, A. Schadschneider, Empirical study on social groups in pedestrian evacuation dynamics, *Physica A* 457 (2017) 129–141.
- [24] A. Garcimartín, I. Zuriguel, M. Pastor, C. Martín-Gómez, D. R. Parisi, Experimental evidence of the “faster is slower” effect, *Transportation Research Procedia* 2 (2014) 760–767.
- [25] R. V. N. Melnik, Dynamic system evolution and markov chain approximation, *Discrete Dynamics in Nature and Society* 2 (1998) Art. 651894.
- [26] R. V. N. Melnik, Markov chain network training and conservation law approximations: Linking microscopic and macroscopic models for evolution, *Applied Mathematics and Computation* 199 (1) (2008) 315–333.
- [27] R. V. N. Melnik, Coupling control and human factors in mathematical models of complex systems, *Engineering Applications of Artificial Intelligence* 22 (3) (2009) 351–362.

- [28] R. Besenczi, N. Bátfi, P. Jeszenszky, R. Major, F. Monori, M. Ispány, Large-scale simulation of traffic flow using Markov model, PLoS ONE 16 (2) (2021) e0246062.
- [29] G. A. Pavliotis, Stochastic Processes and Applications: Diffusion Processes, the Fokker-Planck and Langevin Equations. Texts in Applied Mathematics, Vol. 60, Springer Verlag, Berlin, 2014.
- [30] H. Spohn, Large Scale Dynamics of Interacting Particles, Springer-Verlag Berlin Heidelberg, 1991.
- [31] L. Wilkinson, M. Friendly, The history of the cluster heat map, The American Statistician 63 (2) (2009) 179–184.